Journal of Photochemistry and Photobiology A: Chemistry 210 (2010) 36–43

Contents lists available at ScienceDirect

Journal of Photochemistry and Photobiology A: Chemistry

journal homepage: www.elsevier.com/locate/jphotochem

# Rare earth (Eu/Tb)/phthalic acid functionalized inorganic Si–O/organic polymeric hybrids: Chemically bonded fabrication and photophysical property

Kai Sheng, Bing Yan*, Xiao Fei Qiao, Lei Guo

*Department of Chemistry, Tongji University, Siping Road 1239, Shanghai 200092, China*

ARTICLE INFO

*Article history:*
Received 22 August 2009
Received in revised form
27 November 2009
Accepted 12 December 2009
Available online 21 December 2009

*Keywords:*
Organic/inorganic/polymeric hybrid material
Photophysical property
Rare earth ion
Luminescence

ABSTRACT

The novel rare earth organic/inorganic/polymeric hybrids Eu/Tb–(PHA-Si)–PMMA have been fabricated through chemically bonding assembly technology. The photoactive ligand PHA (O-phthalic anhydride) modified by silane coupling agent APES ((3-aminopropyl) triethoxysilane) is used as a double-functional bridge molecule to link the lanthanide ions and the silica with covalent bonds to form the inorganic Si–O networks. The polymer ligand PMMA (poly methyl methacrylate) is used as the co-ligand coordinating to $Eu^{3+}$ or $Tb^{3+}$ to form the organic polymeric C–C chains, which is prepared through the direct addition polymerization of MMA monomer in the presence of the initiator BPO (benzoyl peroxide). These hybrids are examined by FTIR, TG and luminescence spectra to investigate their composition and photophysical properties. And the luminescence quantum efficiency of the europium hybrids is calculated. Compared to the binary hybrid materials Eu/Tb–(PHA-Si) without organic polymer PMMA, the ternary hybrid materials Eu/Tb–(PHA-Si)–PMMA exhibit stronger luminescence intensities, longer lifetimes and higher quantum efficiency, which indicates the introduction of the organic polymer PMMA bring the improvement on the luminescence property of the hybrid system.



## 1. Introduction

In recent years, luminescent lanthanide-containing (especially Eu, Tb) materials have gained more and more attention for ideal candidates as emitting centers due to their intrinsic properties of lanthanide ions such as narrow emission lines, large Stokes shifts and high quantum efficiency. Since their peculiar $4f^n$ open-shell electronic configuration and the f orbitals are shielded from their environment by outer 5s and 5p electrons, the transition between the states of $4f^n$ configuration is strictly parity forbidden [1]. Thus, the absorption coefficient and the emission intensity are largely restricted. Designing luminescent lanthanide complexes with organic ligands is an interesting area nowadays for that the organic ligand can absorb abundant energy in near-UV region and transfer the excitation energy to lanthanide ions through "antenna effect" [2]. The lanthanide complexes with organic ligands hold large potential applications in many aspects such as fluorescent probes [3], light-emitting diodes [4], biological sensors [5], acidic catalysts [6], and medical magnetic resonance imaging [7]. However, lanthanide complexes have been excluded from practical applications mainly due to their poor thermal stability and low mechanical resistance [8,9]. Many research groups incorporate lanthanide complexes into inert host matrices such as sol–gel glasses [10–14], polymers [15–26], liquid crystals [27,28], or organic–inorganic hybrid materials [29] to overcome these shortcomings. Among these matrices, organic–inorganic hybrid materials with or without polymers have great advantages [30–36].

Organic–inorganic hybrid materials have attracted considerable attention owing to their excellent properties as they combine remarkable mutual features of both organic and inorganic components at molecular level. Immobilization of lanthanide complexes into matrices to obtain organic–inorganic hybrid materials can not only improve the mechanical and thermal stabilities but also avoid self-quenching of the lanthanide ions [37,38]. The critical step to obtain the sol–gel derived molecular based organic–inorganic hybrid materials is how to construct dual-functional molecular bridge which can coordinate to lanthanide ions and covalently bond to silane coupling reagents simultaneously [39,40]. The silane coupling reagent is used to form inorganic Si–O networks via the so-called inorganic polymerization.

Polymers have attractive significance such as low cost, lightweight, tough, easy to fabricate and convenient to control various optical parameters [41,42]. Up to now, there are two methods to incorporate lanthanide complexes into polymers. One is called conventional method or doping method, that is, direct dissolution or dispersion of lanthanide complexes in polymer matrix. Using this method, phase separation and leaching or clustering of

* Corresponding author. Tel.: +86 21 65984663; fax: +86 21 65982287.
*E-mail address:* byan@tongji.edu.cn (B. Yan).

1010-6030/$ – see front matter © 2009 Elsevier B.V. All rights reserved.
doi:10.1016/j.jphotochem.2009.12.008

the photoactive center resulting from the high vibration energy of the surrounding hydroxyl groups often occurred because of the weak physical interaction (such as hydrogen bonding, van der Waals force or electrostatic forces) between lanthanide complex and the polymer. While these problems can be well solved using another method, that is, attach the lanthanide ions to the polymer backbone with covalent bond. That requires the polymer must possess coordinatable groups such as carbonyl, amino and sulfo groups. On the one hand, the polymer coordinates with lanthanide ions which can change the microenvironment of the coordination sphere for example replacement of coordinated water molecule. On another hand, the coordinated polymer can increase the absorption cross-section which is favorable to the ligand–metal energy transfer (LMET). Thus, the high luminescence intensity and long lifetime of the material can be achieved.

In this paper, PHA was used as functionalized ligand for synthesizing the ternary lanthanide (Eu, Tb) organic/inorganic/polymeric hybrid materials Eu/Tb–PHA-Si–PMMA with sol–gel method, since on the one hand it was very active and can be easily modified and on the other hand it is important chemical material which is used mainly in the form of the anhydride to produce other chemicals such as dyes, perfumes, saccharin, phthalates and many others. The binary hybrid materials Eu/Tb–PHA-Si without polymer were prepared as well for comparison. The results show that the ternary polymer-containing hybrid materials exhibit stronger emission intensity, longer lifetime and higher luminescent quantum yield.

## 2. Experimental

### 2.1. Starting materials

(3-Aminopropyl) triethoxysilane was provided by Lancaster Synthesis Ltd., and the tetraethoxysilane (TEOS) by Aldrich. The solvents used were purified by common methods. Other starting reagents were used as received.

### 2.2. The synthesis of the precursor PHASi

O-phthalic anhydride (PHA, 1 mmol) was first dissolved in 15 mL refluxing anhydrous ethanol (EtOH) by stirring, and then 1 mmol (0.018 g) deionized water and 1 mmol NaOH (0.04 g) were added to the solution. Two hours later, 1 mmol (3-aminopropyl) triethoxysilane was put into the solution by drops. The whole mixture was refluxed at 75 °C under argon for 8 h. After isolation of the sample using a rotary vacuum evaporator, a yellow oil PHASi was obtained. It was washed with 20 mL hexane for 3 times and dried in vacuum. Anal. Calcd. for $C_{17}H_{27}O_6NSi$ (369.48): C 55.3, H 7.37, N 3.79; Found: C 55.7, H 7.25, N 3.83. $^1$H NMR ($CDCl_3$, 400 MHz): $\delta$ 0.53(t, 2H, $CH_2$Si, $^3J$ = 9.8 Hz), 1.47 (t, 9H, $CH_3$, $^3J$ = 4 Hz), 1.77 (m, 2H, $CH_2CH_2CH_2$), 3.41 (m, 2H, $NHCH_2$), 3.73 (q, 6H, $SiOCH_2$, $^3J$ = 19.2 Hz), 7.48 (t, 2H, $-C_6H_4$, $^3J$ = 5.6 Hz), 7.76 (m, 2H, $-C_6H_4$), 8.53 (t, 1H, *NH*, $^3J$ = 5.6 Hz). (see Scheme 1).

### 2.3. The synthesis of the binary hybrid material Eu–PHA-Si

PHA-Si was dissolved in dry ethanol (15 mL). Then a certain amount of $Eu(NO_3)_3{\cdot}6H_2O$ (0.3 mmol) was added to the solution with stirring drop by drop. After 2 h, a certain amount of tetraethoxysilane (TEOS) and one drop of diluted hydrochloric acid were put into the solution to promote hydrolysis. The molar ratio of $Eu(NO_3)_3{\cdot}6H_2O$/PHASi/TEOS/$H_2O$ was 1:3:6:24. Then the hybrid material Eu–PHA-Si was obtained after removing the solvent at 80 °C in a few days (see Schemes 1 and 2).

### 2.4. The synthesis of the ternary hybrid material Eu–PHA-Si–PMMA

The similar method was used in this process. When we get the solution of binary coordination complex which was dissolved in the blend-solvents of DMF and EtOH, 0.01 g (0.1 mmol) methyl methacrylate (MMA) was added in with stirring. The volume ratio of the solvents is 1:1 (15 mL for either). Then $5 \times 10^{-4}$ g benzoyl peroxide (BPO) was put into the refluxing mixture at 80 °C. Twelve hours later, a certain amount of tetraethoxysilane (TEOS) and one drop of diluted hydrochloric acid were put into the solution at room temperature to promote hydrolysis. The molar ratio of $Eu(NO_3)_3{\cdot}6H_2O$/PHA-Si/MMA/TEOS/$H_2O$ was 1:3:1:6:24. Then the hybrid material Eu–PHA-Si–PMMA was obtained after removing the solvent at 80 °C in a few days (see Schemes 1 and 2).

### 2.5. Physical measurements

All measurements were performed at room temperature. Infrared spectra were recorded on a Nexus 912 AO439 FT-IR spectrophotometer. We mixed the compound with the dried potassium bromide (KBr) and then pressed into pellets, which were collected over the range 4000–400 $cm^{-1}$ by averaging 32 scans at a maximum resolution of 8 $cm^{-1}$. $^1$H NMR spectra were recorded in $CDCl_3$ on a Bruker AVANCE-500 spectrometer with tetramethylsilane (TMS) as an internal reference. Ultraviolet absorption spectra of these samples ($5 \times 10^{-4}$ mol $L^{-1}$ ethanol solution) were recorded with an Agilent 8453 spectrophotometer. Thermogravimetric trace (TG) was performed on a Netzsch STA 409 at a heating rate of 15 °C/min under nitrogen atmosphere. The ultraviolet–visible diffuse reflection spectra of the powder samples were recorded by a BWS003 spectrophotometer. The fluorescence spectra were obtained on a RF-5301 spectrophotometer equipped with a stable spec-xenon lamp (450 W) as the light source. Luminescent lifetimes were recorded on an Edinburgh FLS 920 phosphorimeter, using a 450 W xenon lamp as the excitation source (pulse width, 3 μs).

## 3. Results and discussion

### 3.1. The characterization for precursor PHA-Si ($^1$H NMR, FT-IR, and UV–vis) and FT-IR for selected terbium hybrids

The presence of the free organic ligand PHA and the precursor PHASi were characterized by $^1$H NMR, IR and UV absorption spectra. As detailed in the synthesis section, $^1$H NMR relative to precursor PHASi is in agreement with the structure. The chemical shifts relative to –OH has not been observed, which indicates the precursor exist in terms of carboxylate not carboxylic acid. The shifts value located at 8.53 ppm is assigned to the –NH– group and the integration of this signal demonstrates the –NH– group not $-NH_2-$ group, which indicates the hydrogen transfer reaction has taken place.

Infrared spectra were shown in Fig. 1I (A for PHA, B for PHASi) examined at room temperature using the dried potassium bromide (KBr) pellets. From the picture, we can see the three peaks located at 1847, 1766 and 1261 $cm^{-1}$ for PHA which is ascribed to the characteristic peaks of phthalic anhydride originated from the stretching vibration $\nu$ (C=O, as), $\nu$ (C=O, s) and $\nu$ (C–O, as) respectively. These peaks disappeared and were replaced by the absorption of carbonyl group (C=O) in carboxylate moiety at 1573 $cm^{-1}$ for PHASi. The peaks at 905 and 712 $cm^{-1}$ correspond to $\delta$ (Ar–H) of PHA. Furthermore, it can be observed that the obvious new broad band centered at 2966, 2923 and 2885 $cm^{-1}$ corresponding to the vibration of methylene groups of APES. In addition, the vibration ($\nu_{C=O}$, 1716 $cm^{-1}$) of carbonyl group in amide group and the stretching vibration ($\upsilon_{C-N}$, 1291 $cm^{-1}$) prove the formation of amide groups

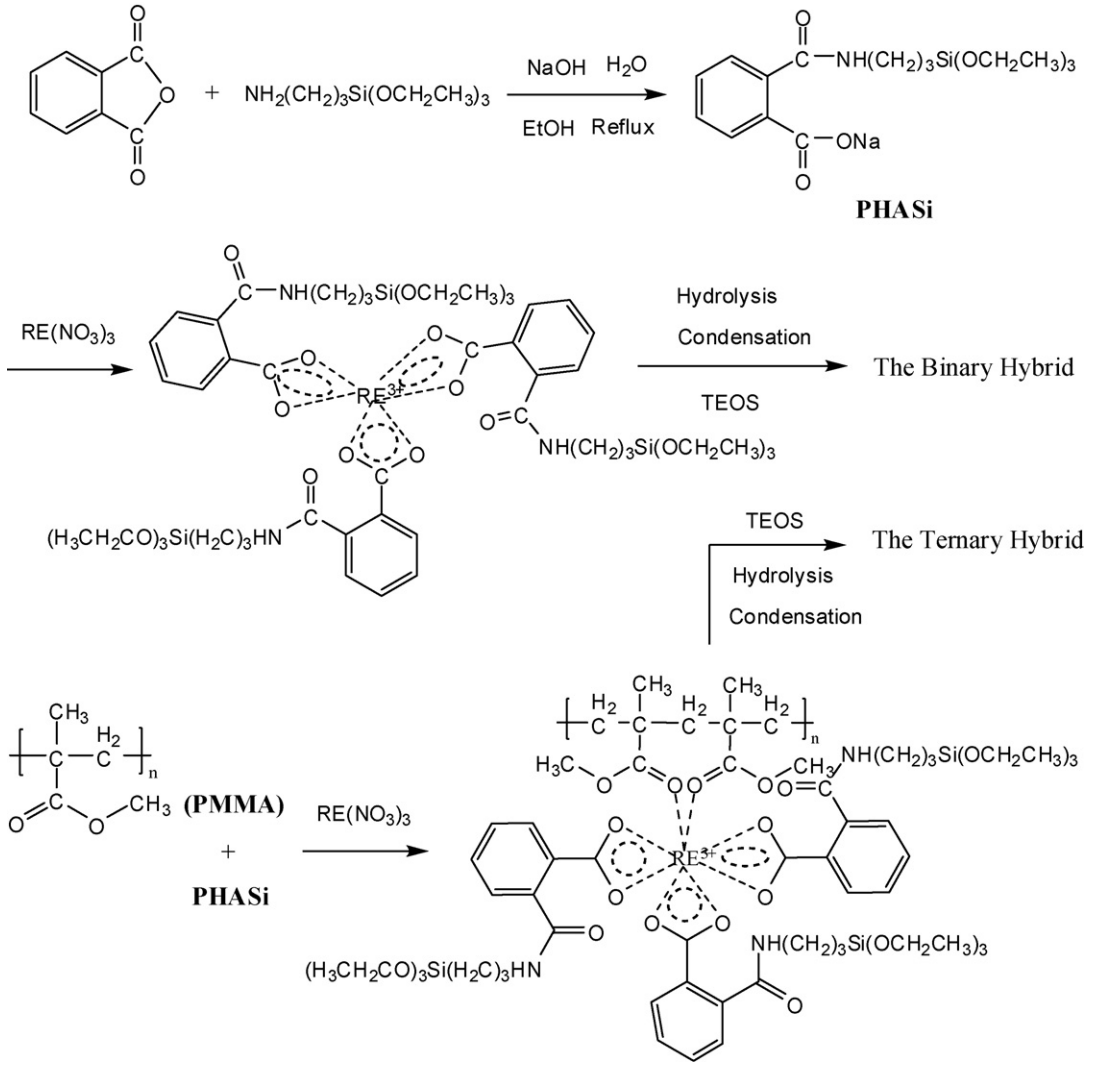


**Scheme 1.** The synthesis route of the binary and the ternary hybrids.

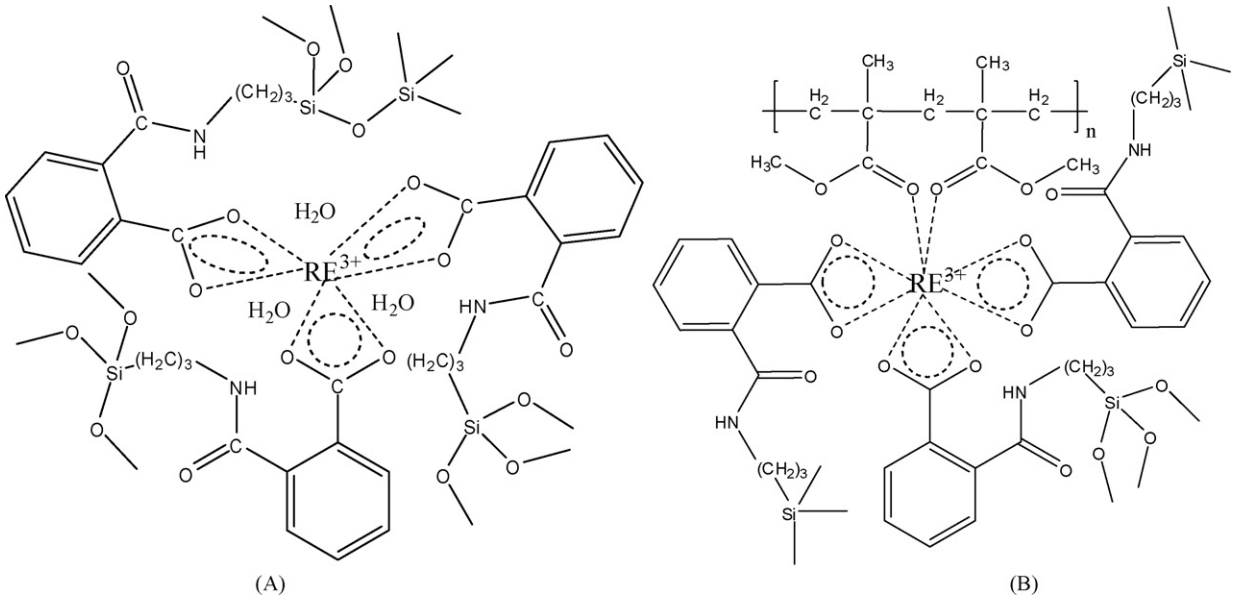


**Scheme 2.** The predicted structure of the binary hybrids (A) and the ternary hybrids (B).

(O═C–NH–), while the strong broad band centered at 3291 $cm^{-1}$ due to the stretching vibration of grafted –NH– groups. The characteristic of trialkoxylsilyl function is evidenced by the broad bands located at 1076 $cm^{-1}$ ($\nu_{as}$, Si–O), 802 $cm^{-1}$ ($\nu_s$, Si–O).

Fig. 1II shows the selected FTIR spectra of the terbium hybrid materials. As can be seen in the picture, the two hybrids exhibit similar plots. The broad band at about 1702 $cm^{-1}$ is ascribed to the low-strength vibration of C═O in amide group and the new peak located at 1645 $cm^{-1}$ is due to the high-strength vibration of C═O in amide group. Further, the strong absorption at 1517 $cm^{-1}$ is assigned to the high-strength bonded carboxylate groups. The sharp peak at 1383 $cm^{-1}$ is the characteristic absorption of free nitrate which show that the nitrate did not coordinate to lanthanide ions. Moreover, the evident peak appearing at 1086 $cm^{-1}$ is due to asymmetric Si–O stretching vibration modes ($\upsilon_{as}$, Si–O) and the peak at 804 $cm^{-1}$ can be attributed to the symmetric Si–O stretching vibration ($\upsilon_s$, Si–O). Additionally, there exists a new peak at 429 $cm^{-1}$ which is corresponding to Tb–O vibration.

Fig. 2 shows the UV absorption spectra of (A) PHA, (B) PHASi. Comparing the two spectra, a blue shift from 210 to 203 nm is ascribed to the major π–π* electronic transitions. This indicates that the electronic conjugating system of the ligand PHA was changed by the introduction of the APES, which can sustain the fact that the coupling reagent was covalently grafted onto the ligand and the precursor was successfully obtained in situ. Additionally, it is observed that the intensity of the absorbency has decreased which may influence the luminescent intensity of the ultimate hybrid material.

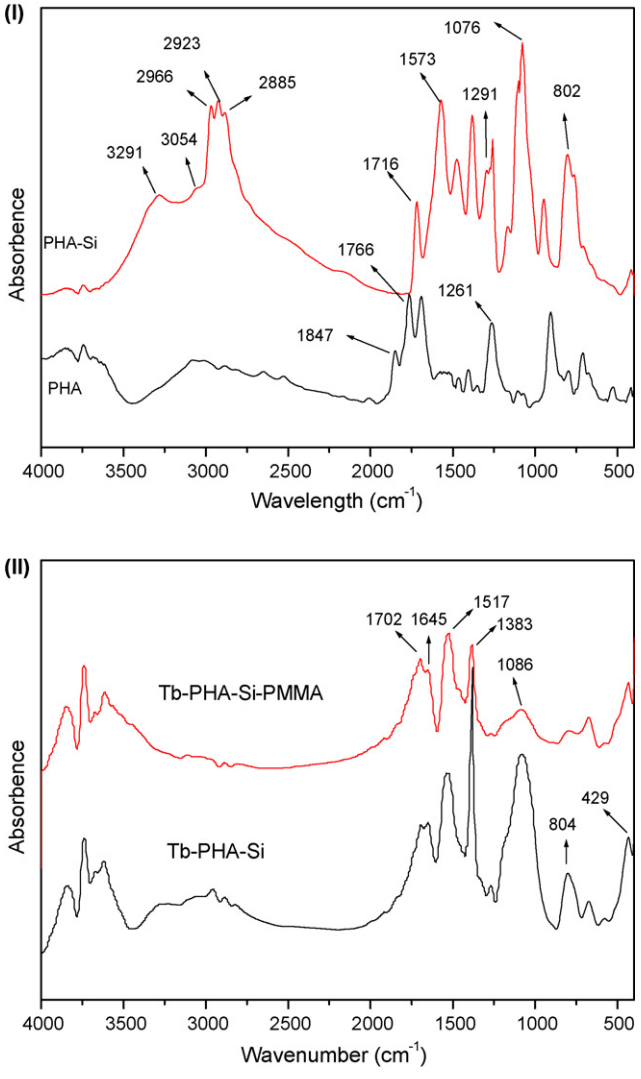


**Fig. 1.** The Fourier transform infrared spectra of the free ligand PHA (I A), the precursor PHASi (IB) and the terbium hybrid materials (II).

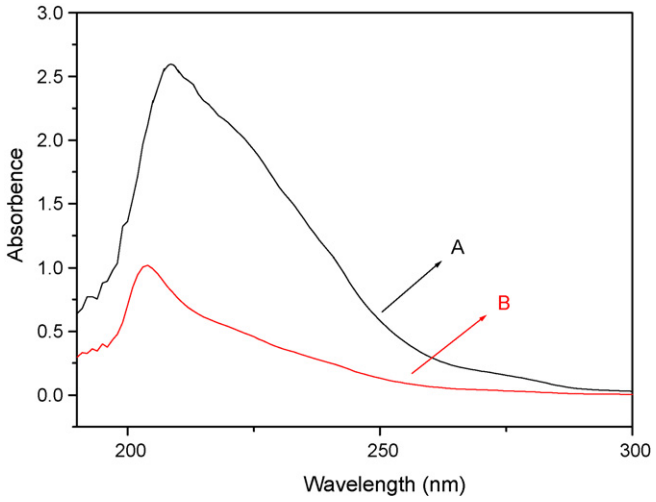


**Fig. 2.** The ultraviolet absorption spectra of PHA (A) and PHASi (B).

### 3.2. Thermal and structural properties of the hybrid materials

The thermogravimetry (TG) trace and differential thermogravimetry (DTG) trace of the hybrid Eu–PHA-Si–PMMA are shown in Fig. 3. Seen from the figure, there are a 5.87% weight loss from 185 °C to 242 °C with the speed 2.88% $min^{-1}$ at 189 °C observed from the DTG curve which is attributed to the loss of the adsorbed and coordinated water molecule and the residual solvent DMF. From 242 °C to 600 °C, a weight loss of totally 34.18% is observed which is ascribed to the decomposition of the organic component of the complicated hybrid. Concomitant with this weight loss, there exhibit two obvious peaks in DTG curve at 311 °C and 402 °C respectively. According to the molecule formula of the hybrid material Eu–PHA-Si–PMMA, the ligand PHASi and the polymer PMMA occupied 33.9% (26.3% and 7.6% respectively) of the whole molecule weight which is close to the overall mass loss value 34.18%. Moreover, this weight loss of the hybrid exhibits three stages as can be observed in the TG curve. It is deduced that the first mass loss 8.60% and the second mass loss 7.83% which show consistent with the two exothermic peaks we discussed above correspond to the

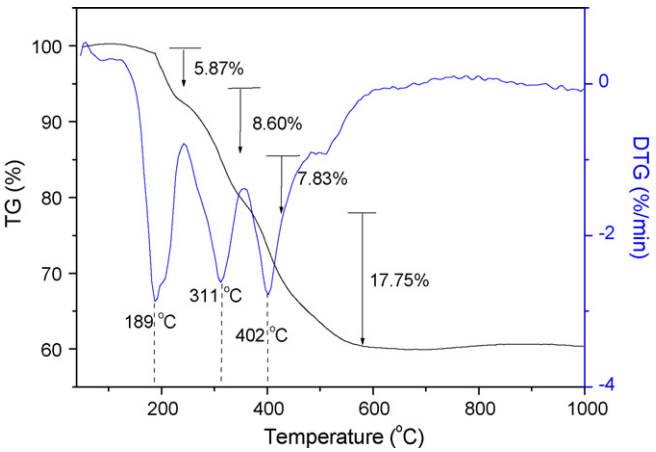


**Fig. 3.** The TG and DTG traces of the hybrid material Eu–PHA-Si–PMMA.

decomposition of organic ligand PHASi and the polymer PMMA, thus the polymer begin to decompose at 326 °C. The third mass loss 17.75% is corresponding to the residual organic ligands. From the view point above, we have calculated the mass loss and the molecular weight to conclude that the molar ration of the PHASi and PMAA is 3:1. Additionally, the hybrids maintain 59.95% mass up to 1000 °C.

### 3.3. The photoluminescence properties of the hybrid materials

The ultraviolet–visible diffuse reflection absorption spectroscopy (UV–vis DRS) of the powdered hybrid materials were measured and displayed in Fig. 4 (A for the europium hybrids and B for the terbium hybrids). It was found that all the hybrid materials exhibit a large broad absorption band from 200 to 550 nm which should be mainly impute to the $\pi$–$\pi^*$ electronic transition of conjugated $\pi$ bond in hybrid system. Besides, the organically modified Si–O network also behaves as host which can produce broad host absorption. For comparison, we measured (UV–vis DRS) the Eu/Tb$(NO_3)_3$. Comparing to the absorption spectra of Eu/Tb$(NO_3)_3$, the absorption bands of the hybrids become stronger and more aboard which reveal that the absorption ability for UV–vis light of the hybrids are better. It is worth noting that there exist some evident inverse peaks (especially for ternary hybrids) centered at 591, 616, 696 nm for Fig. 4A and 545, 583, 620 nm for Fig. 4B which is

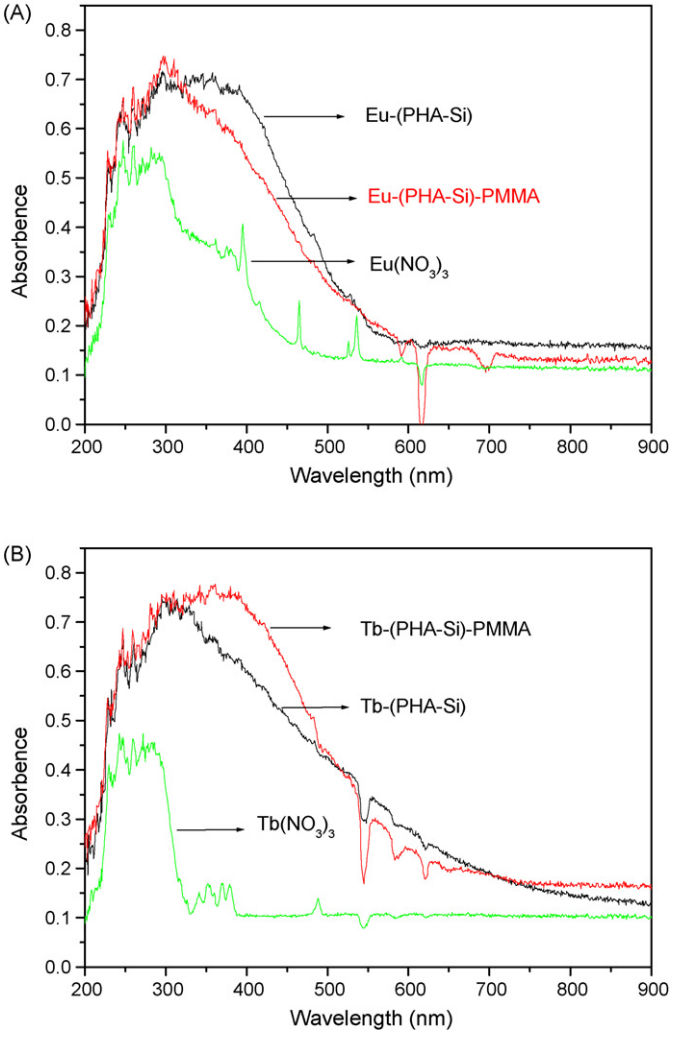


**Fig. 4.** The ultraviolet–vis diffuse reflection absorption spectra of the hybrid materials (A for europium hybrids, B for terbium hybrids).

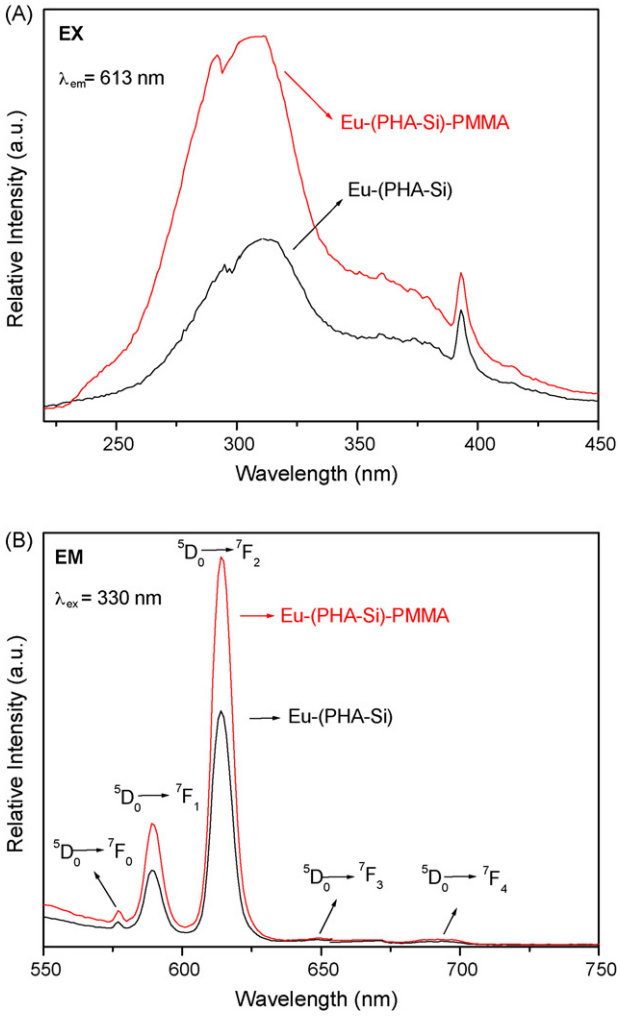


**Fig. 5.** The excitation (A) and emission (B) spectra of the europium hybrid materials.

same position as the characteristic emission lines of europium and terbium ions respectively (as shown in Fig. 5). These inverse peaks are due to the self-absorption of the materials.

The excitation and emission spectra presented in Figs. 5 and 6 are obtained for further investigating the photoluminescence properties of the hybrid materials. The excitation spectra (Figs. 5 and 6A) were obtained by monitoring the maximum emission lines ($^5D_0$–$^7F_2$ for europium hybrids 613 nm, $^5D_4$–$^7F_5$ for terbium hybrids 545 nm). From the excitation spectra, there exists a large broad band in the range of 200–400 nm for each hybrid, which is assigned to the transition of the organic ligands from the ground state $S_0$ to the excited state $S_1$. Moreover, the sharp peak at 393 nm in the excitation spectrum (Fig. 5A) is attributed to the $^7F_0$–$^5L_6$ transition absorbance of $Eu^{3+}$. And there is an obvious blue-shift in Fig. 6A, which indicates that the coordination sphere of the lanthanide ions was changed with the introduction of the organic polymer. Furthermore, all the broad excitation bands overlapped with the absorption bands (Fig. 4) largely, which is sustained the fact that the central lanthanide ions can be well sensitized by the ligands. Figs. 5 and 6B show the room temperature emission spectra of the europium and terbium hybrid materials obtained at the maximum excitation wavelength. For all hybrids, the characteristic $Eu^{3+}$ and $Tb^{3+}$ emissions are observed. As is shown in Fig. 5B, the emission lines for europium hybrid materials obtained from $^5D_0 \rightarrow {}^7F_J$ ($J$ = 0–4) transitions at 577, 589, 614, 648 and 693 nm, respectively under the excitation wavelength at 330 nm.

**Table 1**
The luminescence efficiencies and lifetime data for the hybrid materials.

| Hybrid materials | $\nu_{01}/cm^{-1}$ | $\nu_{02}/cm^{-1}$ | $I_{02}$ | $R(I_{02}/I_{01})$ | $\tau$/ms | $A_r/s^{-1}$ | $A_{nr}/s^{-1}$ | $\eta$/% |
|---|---|---|---|---|---|---|---|---|
| Eu–PHA-Si | 16,978 | 16,287 | 513 | 3.07 | 0.45) | 235 | 1987 | 11 |
| Eu–PHA-Si–PMMA | 16,978 | 16,287 | 847 | 3.16 | 0.87 | 236 | 913 | 21 |

Comparing with the binary organic/inorganic hybrid, the ternary organic/inorganic/polymeric hybrid exhibit stronger luminescence intensity which suggests that the more efficient energy transfer took place between the ligands and the europium ions (antenna effect) and the introduction of the polymer as the co-ligand increased the light absorption cross section. Thus, the presence of the PMMA and the ligands PHA may synergistically sensitize the europium ions. The relative emission intensity of $^5D_0 \rightarrow {}^7F_1$ transition ($I_{01}$) and $^5D_0 \rightarrow {}^7F_2$ transition ($I_{02}$) (red/orange ratio $R$) are listed in Table 1. As is well known, the $^5D_0 \rightarrow {}^7F_1$ transition belongs to the typical electric dipole transition which is hypersensitive to the symmetry of coordination sphere around $Eu^{3+}$ ions. While the $^5D_0 \rightarrow {}^7F_2$ transition is the magnetic dipole transition which is independent of the host materials. Thus, the $R$ value shows importance on judging the symmetry of the microenvironment coordinating the $Eu^{3+}$ as internal standard. From the table, we can see the $R$ value of the hybrids with polymer is higher than the hybrid without organic polymer PMMA, which indicate that the $Eu^{3+}$ occupies a lower symmetry sphere with an inversion center in the presence of PMMA. For terbium hybrid materials (Fig. 6B) the emission lines at 488, 543, 581, 619 nm are assigned to the $^5D_4 \rightarrow {}^7F_J$ ($J$ = 6–3) transitions respectively under their maximum excitation wavelength (330 nm for Tb–(PHA-Si), 313 nm for Tb–(PHA-Si)–PMMA). Among these peaks, the green emission is prominent which indicate the effective energy transfer occurred and the triplet energy level of the ligand PHA-Si can match well with the resonance energy level of the $Tb^{3+}$ ion. While the introduction of the polymer can also increase the luminescence intensity which is consistent with the results of europium hybrids. In the ternary hybrid system, the organic polymer PMMA can coordinate to the lanthanide ions with oxygen atom which can not only increase the coordination number in terms to replacement of water molecule to reduce the non-radiation deactivation resulting from hydroxyl stretching but also increase the absorption cross-section to increase the luminescence intensity. Therefore, the covalent bond of organic polymer PMMA can remarkably increase the luminescence intensity of the hybrids.

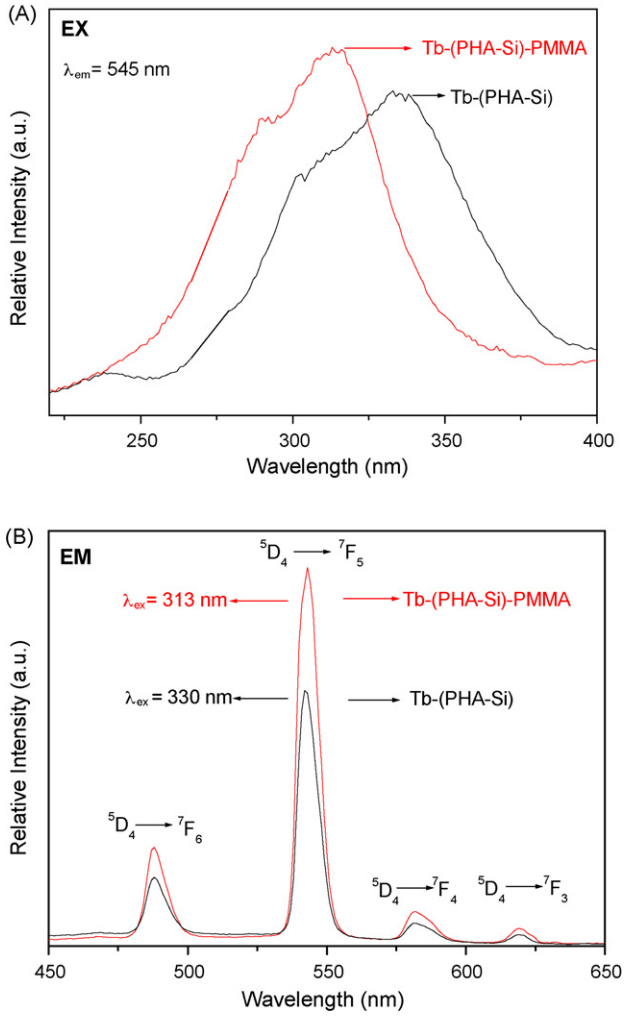


**Fig. 6.** The excitation (A) and emission (B) spectra of the terbium hybrid materials.

### 3.4. Luminescence lifetimes ($\tau$) and emission quantum efficiency ($\eta$)

The decay curves of the hybrid materials obtained by monitoring at the maximum luminescence wavelength fit with a single exponential.

In order to further investigate the photophysical properties of the europium hybrids, the luminescence quantum yield of the $Eu^{3+}$ was calculated based on the emission spectra and the lifetimes of the hybrids and the data obtained by monitoring the main $^5D_0 \rightarrow {}^7F_2$ line were listed in Table 1. The lifetimes of the hybrids can be influenced by Eq. (1) and the quantum yield can be defined as Eq. (2) assuming that only the radiative and nonradiative process occurred during the depopulation of the $^5D_0$ state [43–46]:

$$\tau_{exp} = (A_r + A_{nr})^{-1} \quad (1)$$

$$\eta = \frac{A_r}{A_r + A_{nr}} \quad (2)$$

Here, $A_r$ and $A_{nr}$ denote the radiative and nonradiative transition rates respectively. While $A_r$ can be obtained by summing of each $Eu^{3+}$ $^5D_0 \rightarrow {}^7F_J$ ($J$ = 0–4) transition rates $A_{0J}$:

$$A_r = \sum A_{0J} = A_{01} + A_{02} + A_{03} + A_{04} \quad (3)$$

Since the $^5D_0 \rightarrow {}^7F_{5,6}$ transitions are too weak to be detected by the instrument in the emission spectra, they can be neglected for contribution to Ar. Each transition ratio can be defined as follows [47–50]:

$$A_{0J} = A_{01}\left(\frac{I_{0J}}{I_{01}}\right)\left(\frac{\nu_{01}}{\nu_{0J}}\right) \quad (4)$$

Here, $A_{0J}$ is the experimental coefficient of spontaneous emission. $A_{01}$ is Einstein's coefficient of spontaneous emission between $^5D_0$ and $^7F_1$ energy levels. Since $^5D_0 \rightarrow {}^7F_1$ belongs to the isolated magnetic dipole transition, it is practically independent of the chemical environments around the $Eu^{3+}$ ion, and thus can be considered as an internal reference for the whole spectrum. $A_{01}$ can be determined approximately to be 50 $s^{-1}$ according to Ref. [51]. $I_{0J}$ denotes the emission intensities of $^5D_0 \rightarrow {}^7F_J$ transitions while the $\nu_{0J}$ refers to the wave-number of the emission lines. Additionally,

the emission intensity $I$ can be taken as the integrated intensity $S$ of the $^5D_0 \rightarrow {}^7F_j$ emission bands:

$$I_{i-j} = \hbar\omega_{i-j}A_{i-j}N_i \approx S \quad (5)$$

where $i$ and $j$ are the initial ($^5D_0$) and final levels ($^7F_{0-4}$), respectively, $\omega_{i-j}$ is the transition energy, $A_{i-j}$ is the Einstein's coefficient of spontaneous emission, and $N_i$ is the population of the $^5D_0$ emitting level.

From the view point of the discussion above, the quantum yield $\eta$ of the hybrid is obtained. As can be seen from the table, the lifetimes of the hybrids are 0.45 ms for Eu–PHA-Si, 0.87 ms for Eu–PHA-Si–PMMA, 0.72 ms for Tb–PHA-Si) and 1.04 ms for Tb–PHA-Si–PMMA respectively and the quantum efficiency of the europium hybrids are 11% for Eu–PHA-Si and 21% for Eu–PHA-Si–PMMA respectively. These results confirm that effective energy transfer took place between the polymer PMMA and the lanthanide ions. Besides, it can be seen from the table that the nonradiative deactivation caused by –OH vibration around lanthanide ions decreased apparently comparing the hybrid Eu–PHA-Si–PMMA with Eu–PHA-Si, which revealed the organic polymer PMMA covalently bonded to the lanthanide ions and substituted the coordinated water molecule successfully.

## 4. Conclusions

In summary, we have prepared molecular based organic/inorganic/polymeric hybrid materials Eu/Tb–PHA-Si–PMMA with covalent bonds. Firstly, the precursor PHASi was obtained by modifying the bridge molecule PHA with APES [$NH_2(CH_2)_3Si(OCH_2CH_3)_3$] to form inorganic Si–O networks. The precursor 2 PMMA was obtained through addition polymerization reaction using the monomer MMA to form polymeric C–C chains. Then the two precursors coordinate to lanthanide ions simultaneously. Subsequently, these hybrids containing not only inorganic Si–O network through hydrolysis and condensation process but also organic polymeric C–C chains via polymerization reaction exhibit more excellent properties (especially luminescence properties) than the binary hybrid materials Eu/Tb–PHA-Si with inorganic Si–O network only. The stronger emission intensities and the longer lifetime show that the effective energy transfer took place between the polymer and lanthanide ions. The higher quantum efficiency demonstrates that the polymer PMMA occupied the first coordination sphere of lanthanide ions by replacement of water molecule.

## Acknowledgements

This work was supported by the National Natural Science Foundation of China (20971100) and Program for New Century Excellent Talents in University (NCET-08-0398).

## References

[1] N. Sabbatini, M. Guardigli, J.M. Lehn, Luminescent lanthanide complexes as photochemical supramolecular devices, Coord. Chem. Rev. 123 (1993) 201–228.
[2] J. Coates, P.G. Sammes, R.M. West, Enhancement of luminescence of europium(III) ions in water by use of synergistic chelation. 1. 1:1 and 2:1 complexes, J. Chem. Soc. Perkin Trans. 2 (1996) 1275–1282.
[3] D. Parker, Luminescent lanthanide sensors for pH, pO(2) and selected anions, Coord. Chem. Rev. 205 (2000) 109–130.
[4] S. Capecchi, O. Renault, D.G. Moon, M. Halim, M. Etchells, P.J. Dobson, O.V. Salata, V. Christou, High-efficiency organic electroluminescent devices using an organoterbium emitter, Adv. Mater. 12 (2000) 1591–1594.
[5] G. Mathis, in: R. Saez Puche, P. Caro (Eds.), Rare Earths, Editorial Complutense S.A., Madrid, 1998, p. 285.
[6] E. Emori, T. Arai, H. Sasai, M. Shibasaki, A catalytic Michael addition of thiols to alpha, beta-unsaturated carbonyl compounds: Asymmetric Michael additions and asymmetric protonations, J. Am. Chem. Soc. 120 (1998) 4043–4044.
[7] P. Caravan, J.J. Ellison, T.J. McMurry, R.B. Lauffer, Gadolinium(III) chelates as MRI contrast agents: structure, dynamics, and applications, Chem. Rev. 99 (1999) 2293–2352.
[8] B. Viana, N. Koslova, P. Aschehoug, C. Sanchez, Optical-properties of neodymium and dysprosium doped hybrid siloxane-oxide coatings, J. Mater. Chem. 5 (1999) 719–722.
[9] L.R. Matthews, E.T. Kobbe, Luminescence behavior of europium complexes in sol–gel derived host materials, Chem. Mater. 5 (1993) 1697–1700.
[10] P.A. Tanner, B. Yan, H.J. Zhang, Preparation and luminescence properties of sol–gel hybrid material incorporated with europium complex, J. Mater. Sci. 35 (2000) 4325–4329.
[11] B. Yan, J.Y. You, In-situ sol–gel composition of luminescent hybrid material incorporated with terbium coordination polymers, J. Mater. Proc. Technol. 170 (2005) 363–366.
[12] W. Strek, J. Sokolnicki, J. Legendziewicz, K. Maruszewski, R. Reisfeld, T. Pavich, Optical properties of Eu(III) chelates trapped in silica gel glasses, Opt. Mater. 13 (1999) 41–48.
[13] A.M. Klonkowski, S. Lis, M. Pietraszkiewicz, Z. Hnatejko, K. Czarnobaj, M. Elbanowski, Luminescence properties of materials with Eu(III) complexes: role of ligand, coligand, anion, and matrix, Chem. Mater. 15 (2003) 656–663.
[14] H. Xin, Y. Ebina, R. Ma, K. Takada, T. Sasaki, Thermally stable luminescent composites fabricated by confining rare earth complexes in the two-dimensional gallery of titania nanosheets and their photophysical properties, J. Phys. Chem. B 110 (2006) 9863–9868.
[15] N.E. Wolff, R. Pressley, Optical laser action in an $Eu^{3+}$ containing organic matrix, Appl. Phys. Lett. 2 (1963) 152–154.
[16] Q.M. Wang, B. Yan, Assembly of hybrids from co-polymers bearing functional 4-vinyl pyridine and europium aromatic carboxylates, J. Photochem. Photobiol. A: Chem. 177 (2006) 1–5.
[17] Y. Okamoto, Synthesis, characterization, and applications of polymers containing lanthanide metals, J. Macromol. Sci. Chem. A24 (1987) 455–477.
[18] S. Lin, R.J. Feuerstein, A.R. Mickelson, A study of neodymium-chelate-doped optical polymer waveguides, J. Appl. Phys. 79 (1996) 2868–2874.
[19] H.Y. Chen, R.D. Archer, Synthesis and characterization of linear luminescent schiff-base polyelectrolytes with europium (III) in the backbone, Macromolecules 29 (1996) 1957–1964.
[20] K. Kuriki, Y. Koike, Y. Okamoto, Plastic optical fiber lasers and amplifiers containing lanthanide complexes, Chem. Rev. 102 (2002) 2347–2356.
[21] C.A. Lira, M. Flores, R. Arroyo, U. Caldiño, Optical spectroscopy of $Er^{3+}$ ions in poly(acrylic acid), Opt. Mater. 28 (2006) 1171–1177.
[22] L.D. Carlos, A.L.L. Videira, Emission-spectra and logical symmetry of the Eu3+ ion in polymer electrolytes, Phys. Rev. B49 (1994) 11721–11728.
[23] V.A. Smirnov, O.E. Philippova, G.A. Sukhadolski, A.R. Khokhlov, Multiplets in polymer gels. Rare earth metal ions luminescence study, Macromolecules 31 (1998) 1162–1167.
[24] V. Bekiari, G. Pistolis, P. Lianos, Intensely luminescent materials obtained by combining lanthanide ions, 2,2′-bipyridine, and poly(ethylene glycol) in various fluid or solid environments, Chem. Mater. 11 (1999) 3189–3196.
[25] L.H. Wang, W. Wang, W.G. Zhang, E.T. Kang, W. Huang, Synthesis and luminescence properties of novel Eu-containing copolymers consisting of Eu(III)-acrylate-beta-diketonate complex monomers and methyl methacrylate, Chem. Mater. 12 (2002) 2212–2219.
[26] C.Y. Yang, V. Srdanov, M.R. Robinson, G.C. Bazan, A.J. Heeger, Orienting $Eu(dnm)_3phen$ by tensile drawing in polyethylene: polarized $Eu^{3+}$ emission, Adv. Mater. 14 (2002) 980–983.
[27] K. Binnemans, C. Görller-Walrand, Lanthanide-containing liquid crystals and surfactants, Chem. Rev. 102 (2002) 2303–2345.
[28] R. Van Deun, D. Moors, B. De Fre, K. Binnemans, Near-infrared photoluminescence of lanthanide-doped liquid crystals, J. Mater. Chem. 13 (2003) 1520–1522.
[29] B. Yan, Q.M. Wang, In-situ composition and luminescence of terbium coordination polymers/PEMA hybrid thick films, Opt. Mater. 27 (2004), pp. 555-537.
[30] B. Yan, Q.M. Wang, First two luminescent molecular hybrids composed of bridged Eu(III)–β-diketone chelates covalently trapped in silica and titanate gels, Cryst. Growth Des. 6 (2008) 1484–1489.
[31] B. Yan, H.F. Lu, Lanthanide centered covalently bonded hybrids through sulfide linkage: molecular assembly, physical characterization and photoluminescence, Inorg. Chem. 47 (2008) 5601–5611.
[32] J.L. Liu, B. Yan, Lanthanide ($Eu^{3+}$, $Tb^{3+}$) centered hybrid materials using modified functional bridge chemical bonded with silica: molecular design, physical characterization and photophysical properties, J. Phys. Chem. B 112 (2008) 10898–10907.
[33] J.L. Liu, B. Yan, Molecular construction and photophysical properties of luminescent covalently bonded lanthanide hybrid materials: organic ligands containing 1,2,4-triazole grafted with silica by mercapto modification, J. Phys. Chem. C 112 (2008) 14168–14178.
[34] B. Yan, X.F. Qiao, Rare earth/inorganic/organic polymeric hybrid materials: molecular assembly, regular microstructure and photoluminescence, J. Phys. Chem. B. 111 (2007) 12362–12374.
[35] X.F. Qiao, B. Yan, Assembly, characterization and photoluminescence of hybrids containing europium (III) complexes covalently bonded to inorganic Si–O networks/organic polymers by modified β-diketone, J. Phys. Chem. B 112 (2008) 14742–14750.
[36] X.F. Qiao, B. Yan, Hybrid materials of lanthanide centers/functionalized β-diketone/silicon-oxygen network/polymeric chain: coordination bonded

assembly, physical characterization and photoluminescence, Inorg. Chem. 48 (2009) 4714–4723.
[37] T. Suratwala, Z. Gardlund, K. Davidson, D.R. Uhlmann, Silylated coumarin dyes in sol–gel hosts. 2. Photostability and sol–gel processing, Chem. Mater. 10 (1998) 199–209.
[38] C. Molina, K. Dahmouche, C.V. Santilli, A.F. Craievich, S.J.L. Ribeiro, Structure and luminescence of $Eu^{3+}$-doped class I siloxane-poly(ethylene glycol) hybrids, Chem. Mater. 13 (2001) 2818–2823.
[39] Q.M. Wang, B. Yan, From molecules to materials: a new way to construct luminescent chemical bonded hybrid systems based with ternary lanthanide complexes of 1,10- phenanthroline, Inorg. Chem. Commun. 7 (2004) 1124–1127.
[40] B. Yan, F.F. Wang, Molecular design and photophysics of quaternary hybrid terbium centered systems with novel functional di-urea linkages of strong chemical bonds through hydrogen transfer addition, J. Organomet. Chem. 692 (2007) 2395–2401.
[41] M.I. Sarwar, Z. Ahmad, Interphase bonding in organic-inorganic hybrid materials using aminophenyltrimethoxysilane, Eur. Polym. J. 36 (2000) 89–94.
[42] D. Liu, Z.G. Wang, Novel polyaryletherketones bearing pendant carboxyl groups and their rare earth complexes. Part I. Synthesis and characterization, Polymer 49 (2008) 4960–4967.
[43] J.C. Boyer, F. Vetrone, J.A. Capobianco, A. Speghini, M. Bettinelli, Variation of fluorescence lifetimes and Judd-Ofelt parameters between $Eu^{3+}$ doped bulk and nanocrystalline cubic $Lu_2O_3$, J. Phys. Chem. B 108 (2004) 20137–20144.
[44] S.T. Frey, M.L. Gong, W.D. Horrocks, Synergistic coordination in ternary complexes of $Eu^{3+}$ with aromatic beta-diketone ligands and 1,10-phenanthroline, Inorg. Chem. 33 (1994) 3229–3234.
[45] O.L. Malta, H.J. Batista, L.D. Carlos, Overlap polarizability of a chemical bond: a scale of covalency and application to lanthanide compounds, Chem. Phys. 282 (2002) 21–30.
[46] P.C.R. Soares-Santos, H.I.S. Nogueira, V. Félix, M.G.B. Drew, R.A.S. Ferreira, L.D. Carlos, T. Trindade, Novel lanthanide luminescent materials based on complexes of 3-hydroxypicolinic acid and silica nanoparticles, Chem. Mater. 15 (2003) 100–108.
[47] E.S. Teotonio, J.G.P. Espínola, H.F. Brito, O.L. Malta, S.F. Oliveria, D.L.A. de Foria, C.M.S. Izumi, Influence of the N-[methylpyridyl]acetamide ligands on the photoluminescent properties of Eu(III)-perchlorate complexes, Polyhedron 21 (2002) 1837–1844.
[48] L.D. Carlos, Y. Messaddeq, H.F. Brito, R.A.S. Ferreira, V.D. Bermudez, S.J.L. Ribeiro, Full-color phosphors from europium(III)-based organosilicates, Adv. Mater. 12 (2000) 594–598.
[49] M.F. Hazenkamp, G. Blasse, Rare-earth ions adsorbed onto porous glass: luminescence as a characterizing tool, Chem. Mater. 2 (1990) 105–110.
[50] R.A.S. Ferreira, L.D. Carlos, R.R. Gonçalves, S.J.L. Ribeiro, V.D. Bermudez, Energy-transfer mechanisms and emission quantum yields in $Eu^{3+}$-based siloxane-poly(oxyethylene) nanohybrids, Chem. Mater. 13 (2001) 2991–2998.
[51] M.H.V. Werts, R.T.F. Jukes, J.W. Verhoeven, The emission spectrum and the radiative lifetime of $Eu^{3+}$ in luminescent lanthanide complexes, Phys. Chem. Chem. Phys. 4 (2002) 1542–1548.